

Noteworthy Returns from Titan's Schumann Resonance revealed by HASI-PWA Huygens Instrument

*C. Béghin^a, M. Hamelin^b, R. Grard^c, C. Sotin^d, K. Schwingenschuh^e,
J.J. López-Moreno^f, and R.C. Whitten^g*

^a LPC2E CNRS-Orléans University, Fr. ,

^b LATMOS, University Pierre et Marie Curie, Paris, Fr.

^c RSSD,ESA-ESTEC, The Netherlands,

^d JPL-Caltech, Pasadena, USA,

^e SRI-IWF, Graz, Austria,

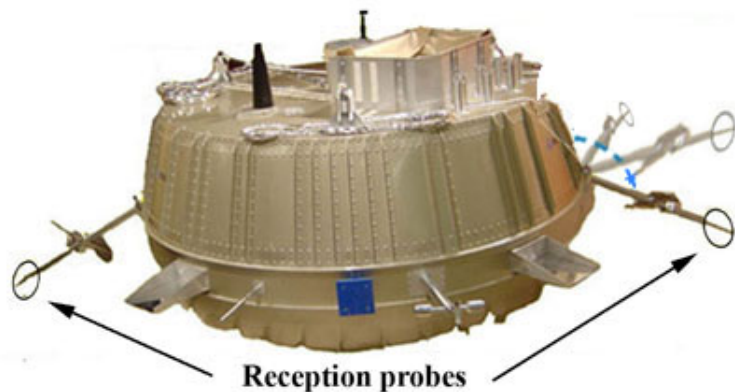
^f IAA-CSIC, Granada, Spain,

^g SETI Institute, Mountain View, USA

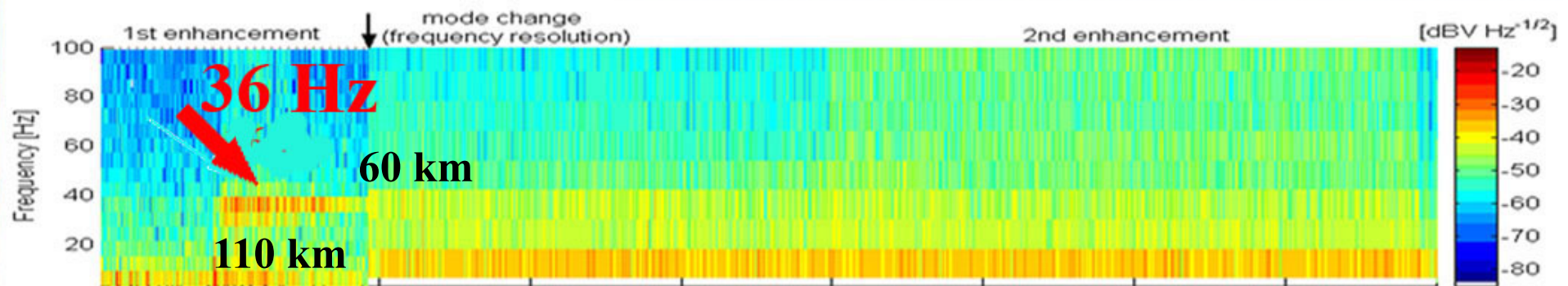
**10 Years After Huygens Landing
Tor Vergata-Rome, January 2015
Cassini PSG # 65 - Titan Workshop II**

HASI-PWA was partly designed to detect lightning activity
and expected radio signals of Schumann Resonance

About thunderstorms & lightning : None were detected since 2005 ...

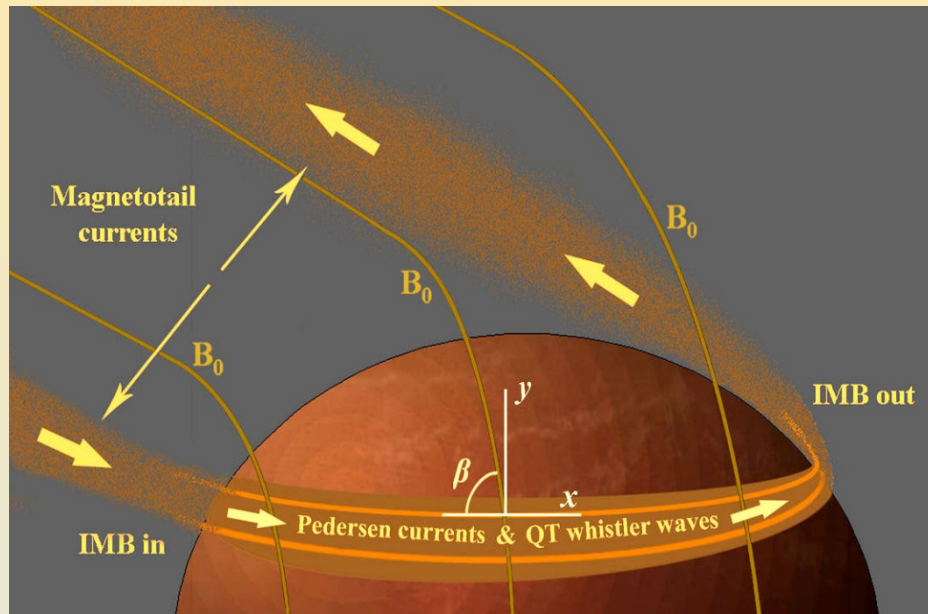


.. but the Schumann Resonance was there
in spite of some instrumental troubles !



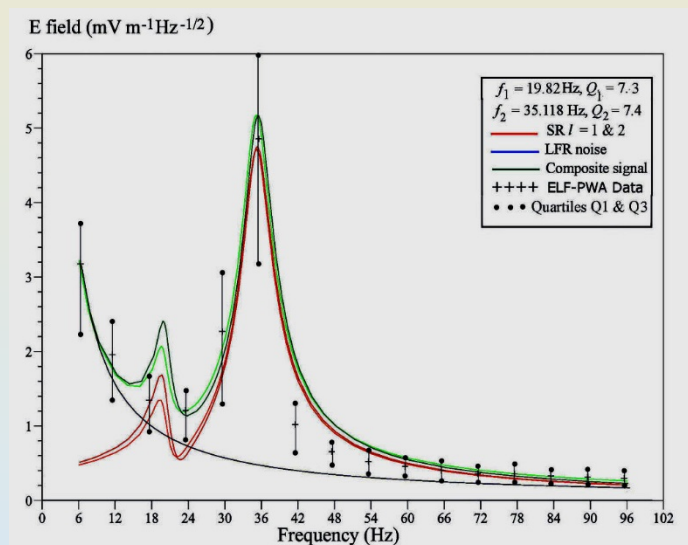
Generation Mechanism of Titan's Schumann Resonance (SR)

-- In the absence of lightning --



Energy source

- Interaction of Saturn's Magnetosphere plasma flow with Titan's Ionosphere
- Ram-side induced Pedersen currents
- $J = \sigma_p E > 2000 \text{ A} \rightarrow J/n_e q_e > C_s$
- Low Frequency Ion-acoustic Instability
- ELF modulated sheets \rightarrow EM antennae



Constraints from the data

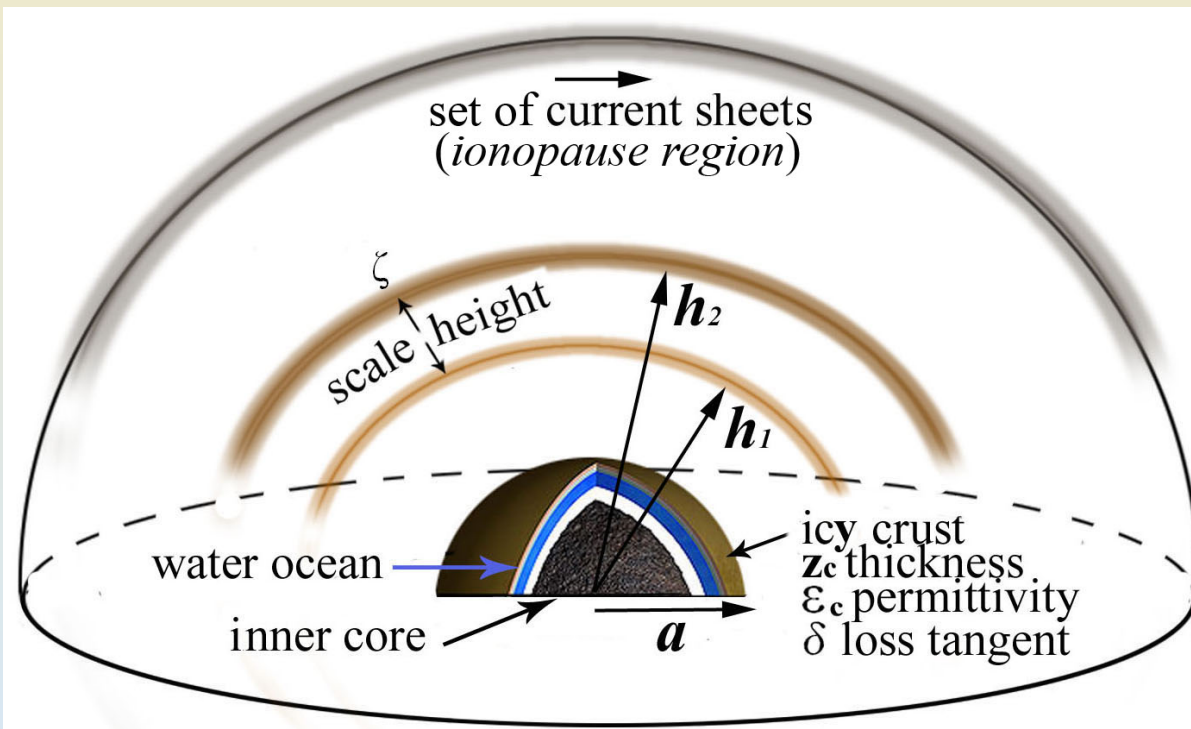
- Because the actual spectral frequency resolution was half of nominal, only the parameters of the 2nd mode are determined with a 75% confidence level.
- $F_{\text{max}} = 35.5 \pm 0.5 \text{ Hz}$, Quality factor $Q = 6.5 \pm 0.5$
- Field amplitude max: $5.5 \text{ mV/m}/\sqrt{\text{Hz}}$ at 100 km altitude
- (excerpt from Béghin, JGR-Planets, 2014).

Constraints on the SR cavity derived from Modal Equations

Inputs : $f = 36$ Hz, $Q = 6$, mode index $l = 2$

$$\omega_l = \frac{c}{a} \left[l(l+1) \frac{h_1 + z_c / R_e \epsilon_c}{h_2 + z_c} \right]^{1/2} \left[1 - i \left(\frac{z_c \delta / R_e \epsilon_c + \pi \zeta / 4}{h_1 + z_c / R_e \epsilon_c} + \frac{\pi \zeta / 4}{h_2 + z_c} \right) \right]$$

$$Q_l = \left| \frac{R_e f_l}{2 I_m f_l} \right| = \left[\frac{2 z_c \delta / R_e \epsilon_c + \pi \zeta / 2}{h_1 + z_c / R_e \epsilon_c} + \frac{\pi \zeta / 2}{h_2 + z_c} \right]^{-1}$$



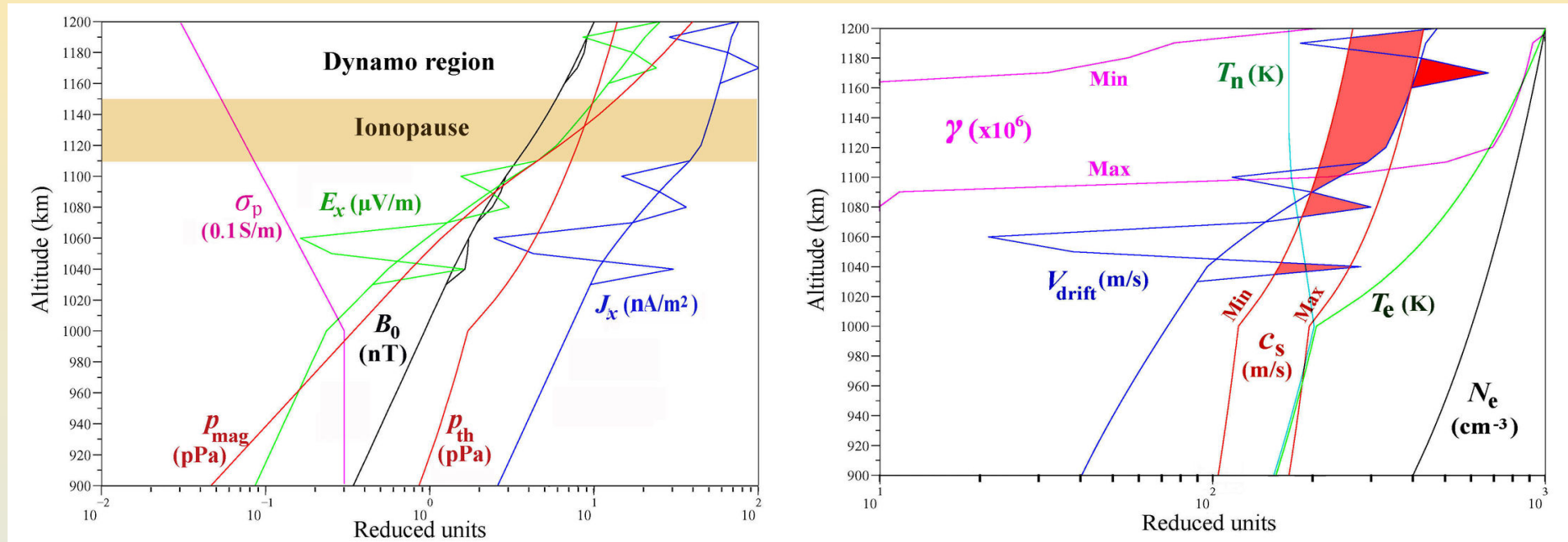
Cavity parameters

- *Atmosphere*
- Conduction boundary: h_1
- Diffusion boundary: h_2
- Conductivity scale height: ζ
- *Surface icy crust*
- -- thickness : z_c
- -- permittivity : ϵ_c
- -- loss tangent : δ
- *Water ocean*
- Highly conductive

(Béghin et al., Icarus 2012)

Constrained Atmospheric Parameters

- 1- Source Region : Data & Models Profiles

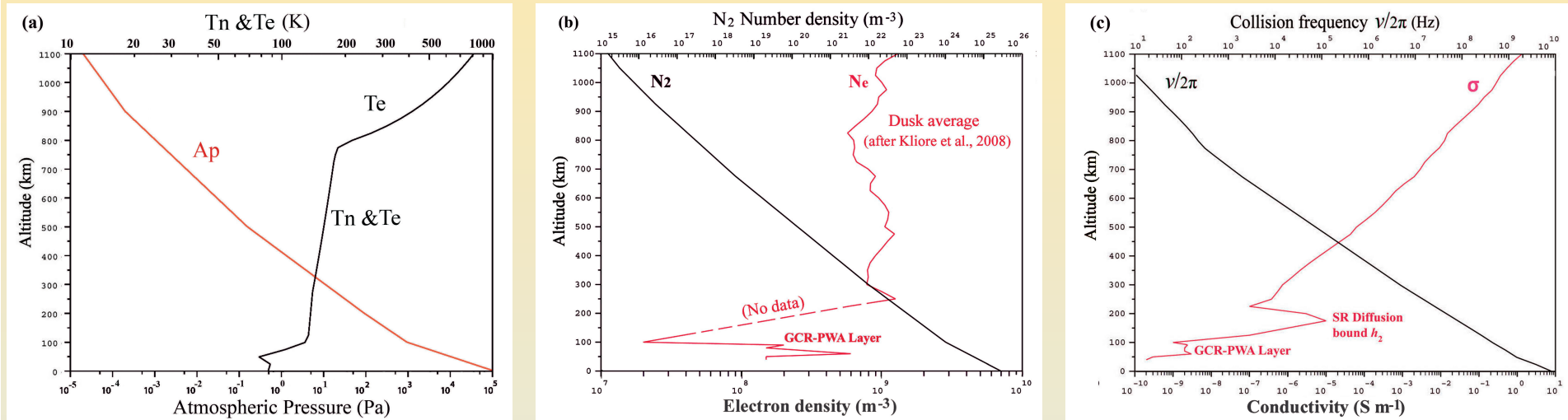


Probable conditions during Huygens descent, derived from regular CASSINI Data

- Huygens descent occurred at middle Latitude daylight ram-side hemisphere
- A bipolar configuration similar to TA-TB-T3 flybys is assumed (*Simon et al., 2013*)
- Plasma and magnetic field profiles are from RPWS & MAG typical published data.
- Current sheet models are derived from reported data (e.g., *Ågren et al., 2011*)
- The region of largest ion-acoustic growth-rate (γ) is highlighted in red (*right panel*).

Constrained Atmospheric Parameters

- 2 - Ionosphere-Atmosphere Data & Models Profiles



Panel (a)

Atmospheric Pressure & Neutral Gas Temperature, from HASI (*Fulchignoni et al., Nature, 2005*)
Electrons supposedly thermalized ($T_e \sim T_i \sim T_n$) below 800 km, starting from 1000 K at 1100 km.

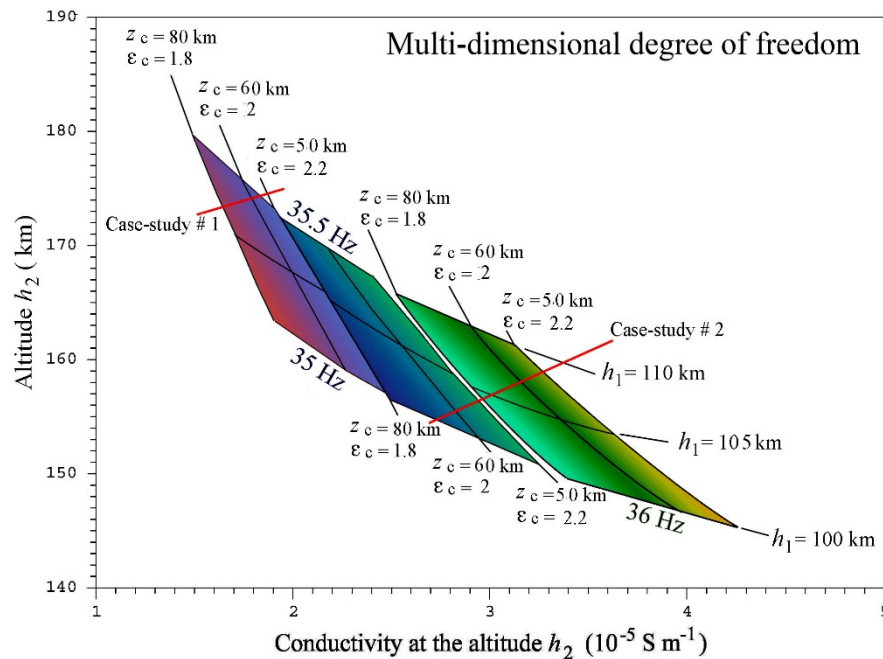
Panel (b)

Neutral gas (N_2) density from HASI,
Electron density (N_e) from 1100 to 250 km from Radio Occultation (*Kliore et al., JGR, 2008*),
 N_e from PWA-HASI below ~ 105 km to surface (*Hamelin et al., PSS, 2007*), 110-250 km no data.

Panel (c)

Electron collision frequency ($\nu/2\pi$) & conductivity (σ) derived from PWA-HASI below 110 km, constrained by SR conduction-diffusion boundaries and aerosols photoemission threshold up to 160 km (*Mishra et al., Icarus, 2014*), furthermore derived from N_e , N_2 and T_e profiles.

Constrained Structure & Physical Properties of the Subsurface

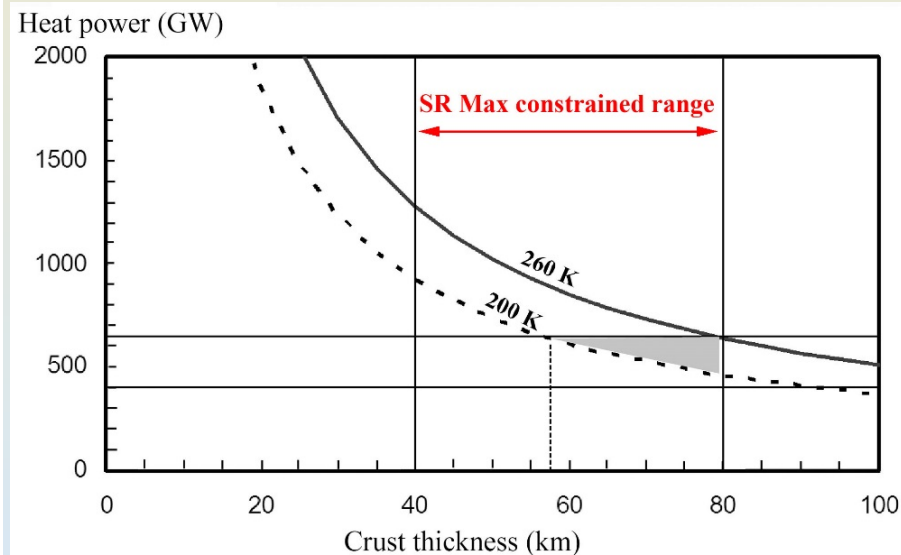


Linked atmosphere-crust constraints

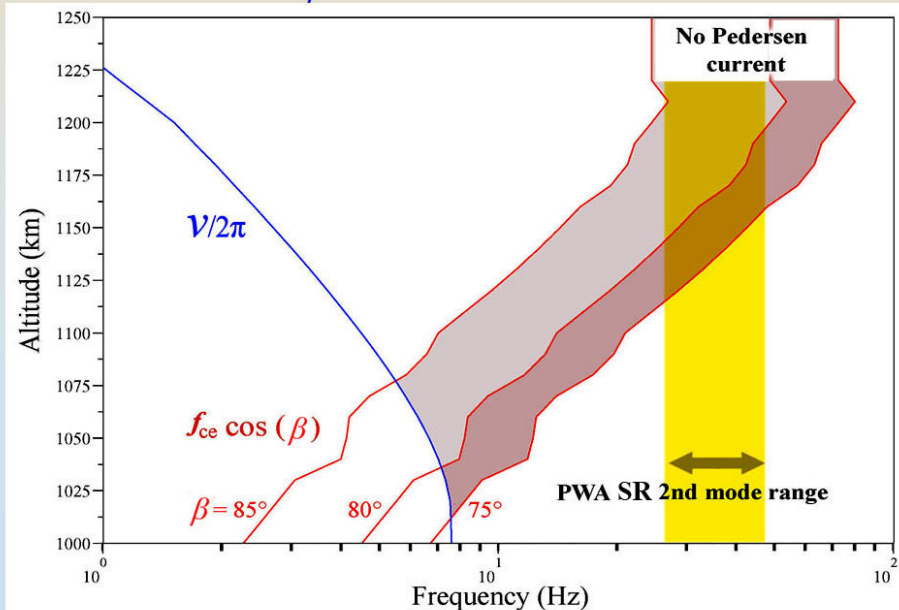
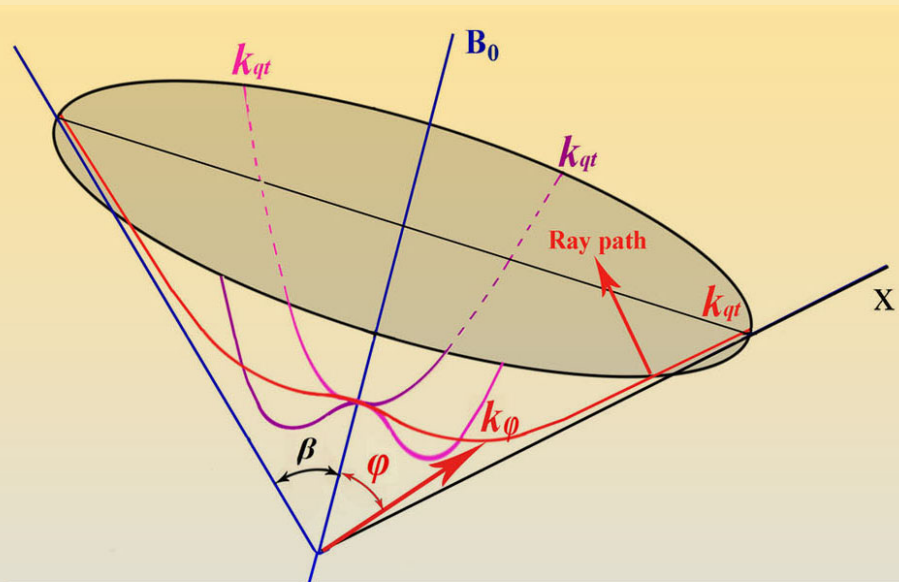
- Crust thickness and permittivity are linked to both atmospheric boundaries (h_1 & h_2) by the modal equation for SR frequency ranging from 35.5 to 36.5 Hz.
- For instance, the degree of freedom is such as z_c is ranging from ~ 40 to 80 km for $1.8 > \epsilon_c > 2.2$, whatever atmospheric boundaries (Mishra et al., Icarus, 2014).

Independent constraints on the crust

- Assuming a core heat power flux range 400-650 GW (Grasset et al., PSS, 2000)
- A flux of 650 GW implies interface ocean temperature max of 260 K (pure ice)
- Presence of ammonia in the ocean would decrease the temperature down to 200 K, reducing accordingly $58 < z_c < 80 \text{ km}$.



Ion-Acoustic Turbulence & Whistler Modes Coupling



excerpt from Béghn, JGR-Planets, 2014

Merged Dispersion Equations

- Equality of both wave vectors

$$k_{ia} = \omega_{ia} / c_s =$$

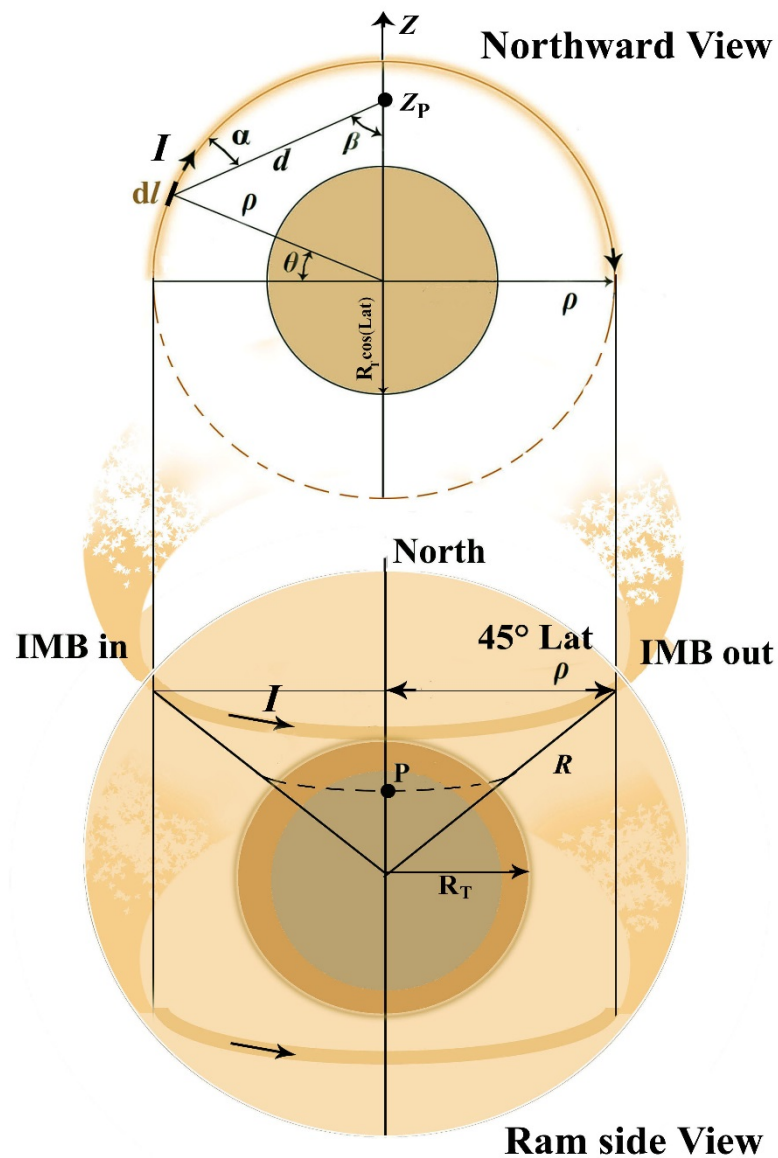
$$k_{qt} = \frac{\omega_{qt}}{c} \left(1 + \frac{\omega_p^2 / \omega_{qt}^2}{\omega_{ce} \cos \beta / \omega_{qt} - 1 + i\nu / \omega_{qt}} \right)^{1/2}$$

- The resulting wave is a quasi-transverse whistler mode, the ray path of which is nearly parallel to magnetic field lines
- The self saturation of the ion-acoustic instability yields the ELF modulation of the current sheets acting as antennas.

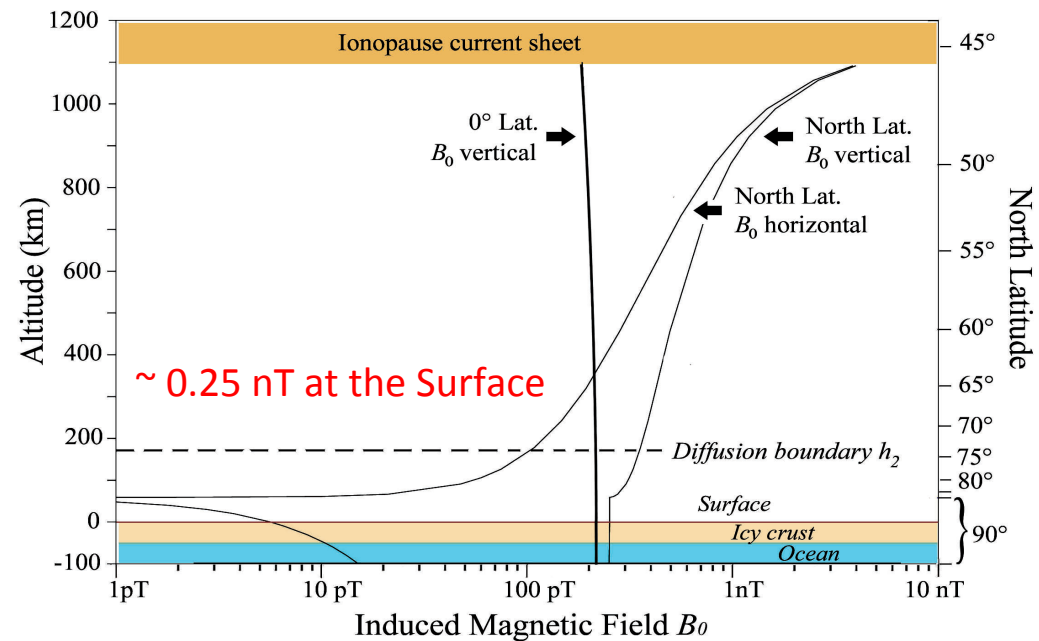
Permitted SR Bandwidth

- The ES-EM coupling mechanism in the SR source region is only possible within a range of oblique resonance constrained by the width of the dip angle β between B_0 and the current sheet.

Secondary Magnetic Field induced in the Atmosphere



(after Béghin, Icarus, 2015)



- The current-induced magnetic field in the atmosphere is derived from Biot-Savart law

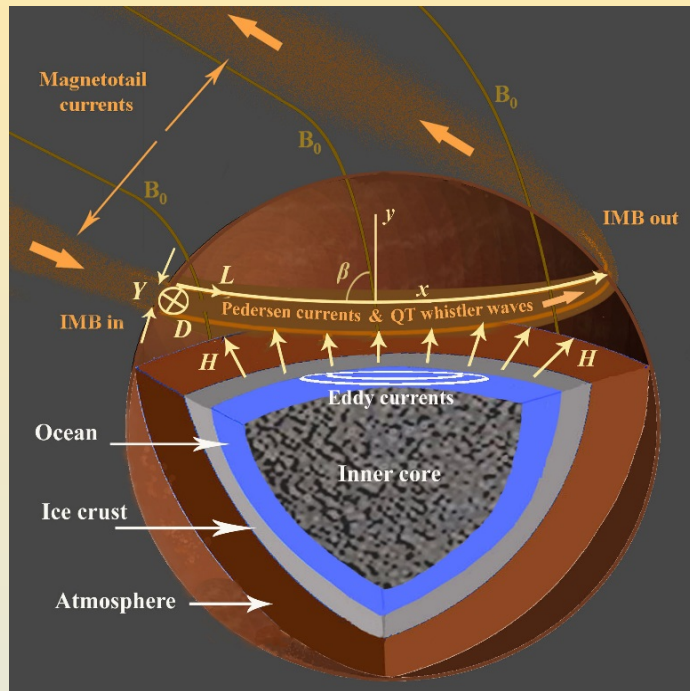
$$d\mathbf{H} = \frac{I dl \sin(\alpha)}{4\pi d^2} \mathbf{u}; \text{ with } \mathbf{u} = d\mathbf{l} \times \mathbf{d},$$

$$\mathbf{B}_0(Z_P) = \frac{\mu_0 I}{4\pi} \int_0^{180^\circ} \frac{\sin(\alpha) \rho d\theta}{d^2} \mathbf{u},$$

- $J \sim 30 \text{ nA/m}^2 \rightarrow I = Y D \bar{J}_x \approx 2100 \text{ A}.$
- ELF modulation : (Kuo et al. GRL, 1999) :

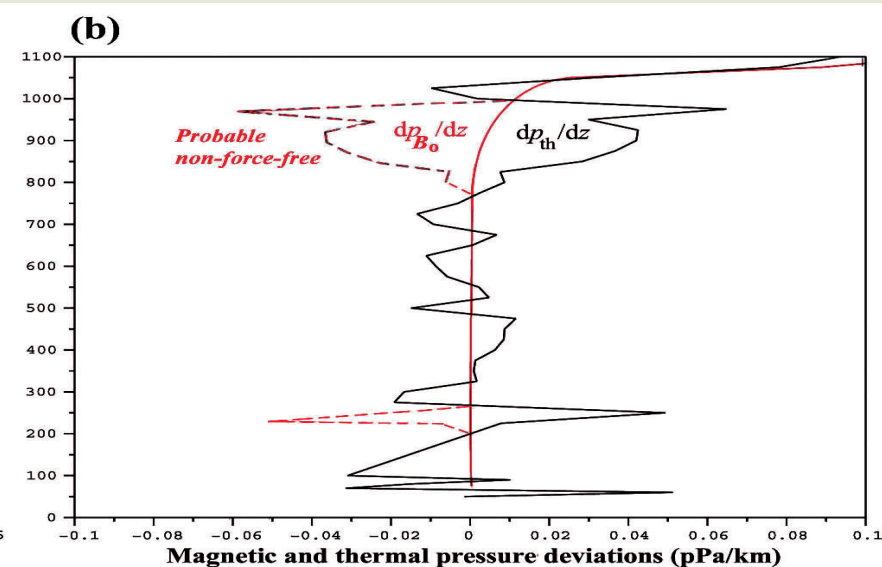
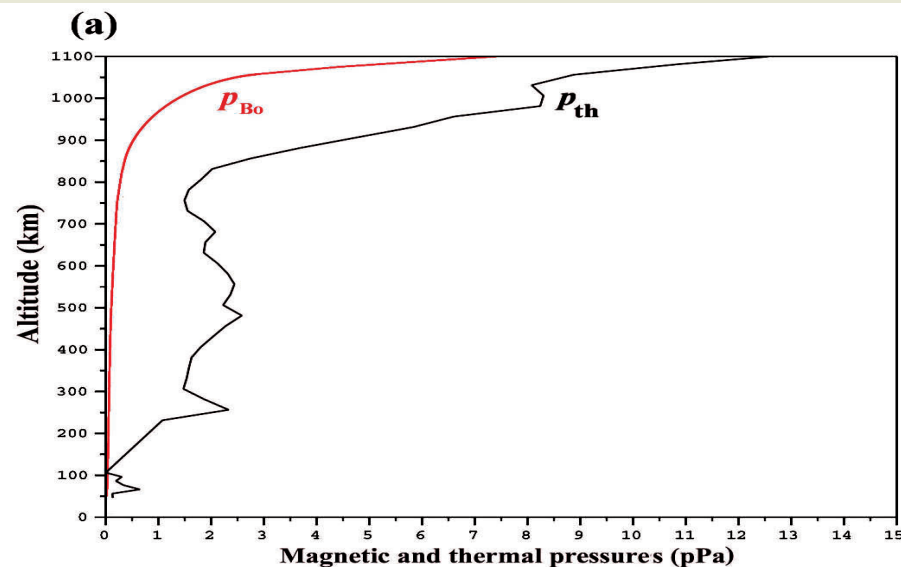
$$\bar{I}(\omega, t) = I \left[1 + \sum_{\omega} \delta_{\omega} (\exp(\pm i \omega t)) \right]$$

Induced DC-ELF Magnetic Field Strength in the Atmosphere



- With a saturation modulation rate $\Delta B/B_0$ of $0.41 \text{ Hz}^{-1/2}$, the value of B_0 at 100 km ($\sim 0.13 \text{ nT}$) is found consistent with the EM strength of the SR signal.
- The vertical ELF modulated field lines are anticipated to induce Eddy-Foucault currents in the buried ocean.
- From MHD assessment of B_0 field force balance, most parts of the altitude profile are found force-free, except between 850-1000 km where a relaxation of about 3.5 nT amplitude could account for a few tens of minutes decay of a retentive “fossil” field such as observed during the T32 flyby.

(Béghin, *Icarus*, 2015) & (Bertucci et al., *Science*, 2008).



Summary

- After the confirmed absence of any detectable lightning activity in Titan's atmosphere, the only conceivable generation mechanism of Titan's Schumann Resonances comes from sets of ionopause current sheets induced by Saturn's magnetosphere interaction.
- A day-light/ram-side atmospheric profile model applicable to Huygens descent is constrained by the Modal Equations of the observed 2nd SR Eigenmode.
- The same method allows to constrain the thickness and the average permittivity of the icy crust, and to reveal the presence of a liquid water ocean buried from 60 to 80 km below the surface.
- The model accounts for the observation of the 2nd mode only, because the meridional orientation of Saturn's magnetic field at the Titan's interface during bi-polar conditions.
- The strength of secondary magnetic field induced in the atmosphere by the current sheets is decreasing from a few nT at 1000 km down to about 0.3 nT at 200 km altitude, extending far beneath the surface and the buried ocean.
- The fleeting remanence of this magnetic field after Titan would have left the Saturn's magnetosphere could explain the existence of a "fossil" field observed in such a case.

- Ågren, K., and 15 colleagues. 2011. Detection of currents and associated electric fields in Titan's ionosphere from Cassini data, *J. Geophys. Res.*, 116.
- Béghin, C., and 8 colleagues. 2012. Analytic theory of Titan's Schumann resonance: Constraints on ionospheric conductivity and buried water ocean, *Icarus*, 218, 1028-1042.
- Béghin, C. 2014. The atypical generation mechanism of Titan's Schumann resonance, *J. Geophys. Res. Planets*, 119, 520-531.
- Béghin, C. 2015. Self-consistent modeling of induced magnetic field in Titan's atmosphere accounting for the generation of Schumann resonance, *Icarus*, 247, 126-136.
- Bertucci, C., and 11 colleagues. 2008. The magnetic memory of Titan's ionized atmosphere, *Science*, 321, 1475-1478.
- Fulchignoni, M., and 42 colleagues. 2005. Titan's physical characteristics measured by the Huygens Atmospheric Structure Instrument (HASI). *Nature* 438, 785–791.
- Grasset, O., Sotin, C., Deschamps, F. 2000. On the internal structure and dynamics of Titan, *Planet. Space Sci.*, 48, 617-636.
- Hamelin, M., and 17 colleagues. 2007. Electron conductivity and density profiles derived from the mutual impedance probe measurements performed during the descent of Huygens through the atmosphere of Titan, *Planet. Space Sci.*, 55, 1964-1977.
- Kliore, A.J., and 12 colleagues. 2008. First results from the Cassini radio occultations of the Titan ionosphere, *J. Geophys. Res.*, 113, A09317.
- Kuo, S.P., Koretzky, E., Lee, M.C. 1999. A new mechanism of whistler generation by amplitude modulated HF waves in the polar electrojet, *Geophys. Res.* 113, A09317.
- Mishra, A., Michael, M., Tripathi, S.N. and Béghin, C. 2014. Revisited modeling of Titan's middle atmosphere electrical conductivity, *Icarus*, 238, 230-240.
- Simon, S., et al. 2013. Structure of Titan's induced magnetosphere under varying background magnetic field conditions: survey of Cassini magnetometer data from flybys TA-T85, *J. Geophys. Res. Space Phys.*, 118, 1679-1699.